Journal of Applied Polymer Science

High-Tensile-Strength Polyvinyl Alcohol Films Prepared from Freeze/Thaw Cycled Gels

Taishi Fukumori, Takahiko Nakaoki
Department of Materials Chemistry, Ryukoku University, Seta, Otsu 520-2194, Japan
Correspondence to: T. Nakaoki (E-mail: nakaoki@rins.ryukoku.ac.jp)

ABSTRACT: The mechanical properties and molecular structure of a poly(vinyl alcohol) (PVA) film, which was obtained by eliminating water from a PVA hydrogel using repeated freeze/thaw cycles, were investigated by tensile tests, thermal analysis, and X-ray diffraction measurements. The mechanical properties of PVA with 99.9% saponification were measured as a function of the number of freeze/thaw cycles performed. The tensile strength and Young's modulus increased and the elongation at break decreased with increasing freeze/thaw cycles. The tensile strength and Young's modulus of PVA films obtained after seven freeze/thaw cycles were as high as 255 MPa and 13.5 GPa after annealing at 130°C. Thermal analysis and X-ray diffraction measurements revealed that this is because of a high crystallinity and a large crystallite size. A good relationship between the tensile strength and the glass transition temperature was obtained, regardless of the degree of saponification and annealing conditions. © 2014 Wiley Periodicals, Inc. J. Appl. Polym. Sci. **2014**, *131*, 40578.

KEYWORDS: films; mechanical properties; morphology

Received 12 December 2013; accepted 11 February 2014
DOI: 10.1002/app.40578

INTRODUCTION

Poly(vinyl alcohol) (PVA) is a water soluble polymer that forms a crystal through hydrogen bonding, even without stereoregularity. Its mechanical properties depend not only on the molecular structure, but also on the addition of additives such as inorganic compounds. There are many reports on the mechanical properties of PVA films. PVA with a saponification of 98–99% annealed at 130°C can have a tensile strength as high as 137 MPa.[1] The addition of Ag,[2] aminoclay and Ag,[3] and graphene[4] can improve the tensile strength of PVA with 98% saponification from 20, 28, and 17 MPa to 60, 72, and 42 MPa, respectively. For PVA with a saponification of over 99%, the addition of polyvinyl pyrolidone (PVP)/sodium dodecyl sulfate (SDS)/single-wall carbon nanotubes (SWNTs)[5] and nanodiamond[6] was reported to improve the tensile strength from 83 and 95 MPa to 148 and 124 MPa, respectively. Significant improvement of the mechanical properties of PVA films was recently reported after using Na^+-montmorillonite+Cu^{2+} [7] and nanodiamond+SWNTs,[8] with which the tensile strength reached 320 MPa (original PVA: 40 MPa) and 534.3 MPa (38.0 MPa), respectively.

PVA forms a stable hydrogel by physical cross-linking. It has been reported that repeatedly freezing at −20°C followed by thawing at room temperature provides a thermoreversible hydrogel.[9,10] The PVA hydrogel is characterized by the aggregation of water, swollen amorphous water-containing PVA, and crystalline PVA at a cross-linking point,[11–15] and the crystallinity increased with increasing freeze/thaw cycles.[13] Transmission electron microscopy (TEM) showed that the aggregated water had a diameter of 30 nm.[16] Thermodynamic analysis was used to obtain additional information on the size of the aggregated water,[17,18] indicating that the diameter was 30.2 nm after two freeze/thaw cycles, which is comparable with the TEM results.

In our previous report, PVA film with 98.5% saponification was prepared from a freeze/thaw cycled gel, and the mechanical properties of this film were investigated.[19] The tensile strength increased with increasing freeze/thaw cycles, from 28.3 MPa after one cycle to 46.2 MPa after 10 cycles. When the 10-cycle film was annealed at 130°C, its tensile strength reached 181 MPa.

In this report, the mechanical properties that depend on the degree of saponification were investigated first. The improvement of the mechanical properties in PVA with a high degree of saponification is discussed after examining films prepared from gels subjected to various numbers of freeze/thaw cycles.

EXPERIMENTAL

Sample Preparation

PVA with a saponification of 95.8 (PVA95.8), 98.5 (PVA98.5), 99.3 (PVA99.3), and 99.9 (PVA99.9) mol % was provided by

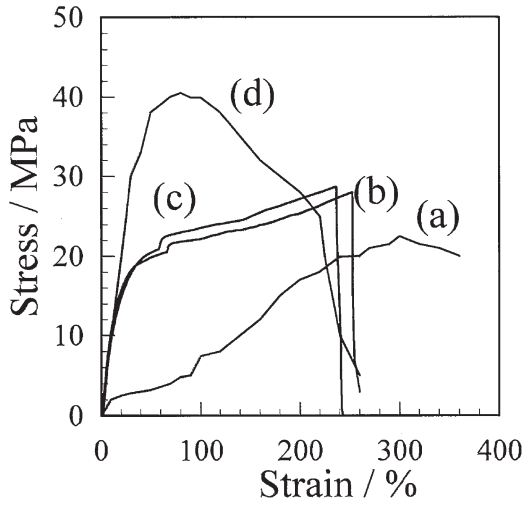

Figure 1. Typical stress–strain curves for PVA with degrees of saponification of (a) 95.8%, (b) 98.5%, (c) 99.3%, and (d) 99.9%. These films were prepared by casting from aqueous solution.

Kuraray. A PVA cast film (CastFx: x denotes the saponification) was formed by casting a 10 wt% PVA solution and drying at room temperature for one week. A film was prepared using a freeze/thaw cycle process as follows. About 10 wt % PVA was dissolved in water at 120°C in an autoclave, and a PVA hydrogel was formed by freezing this solution at −20°C for 5 min and then thawing at 25°C for 45 min. Between one and ten freeze/thaw cycles were employed. The gel was dried at room temperature for one week in vacuum. This film is abbreviated as gel film(n) (GelFx(n)), where n denotes the number of freeze/thaw cycles. Annealing was carried out at 130°C for 30 min in a thermostatic oven; the annealed cast and gel films are abbreviated as aCastFx and aGelFx(n), respectively.

Measurements

Differential scanning calorimetry (DSC) was performed on a Rigaku 8230D instrument at a heating rate of 5°C/min from room temperature to 250°C.

The mechanical properties were measured using a tensile testing instrument (Shimadzu Instron 5566), with a head speed of 0.5 mm/min. The PVA test samples had a lateral shape, with dimensions of a length of 3.0–4.0 cm, a width of 1.0–1.5 cm, and a thickness of 0.1–0.3 mm. At least three tensile measurements were conducted for each set of conditions, and the average value was adopted. Young's modulus was estimated by the initial slope of stress–strain curve.

Dynamic mechanical analysis (DMA) was performed on a dynamic viscoelasticity instrument (I.T. Instruments DVA-200). The heating rate was 3°C/min from −100°C to 200°C. The glass transition temperature (T_g) was determined from the initial temperature required to decrease the storage modulus.

RESULTS AND DISCUSSION

Mechanical Property Dependence on Saponification

The degree of saponification is an important factor determining physical properties, so the mechanical properties of cast films with four different degrees of saponification were compared. Stress–strain curves of CastF95.8, CastF98.5, CastF99.3, and CastF99.9 are shown in Figure 1. The tensile strength, Young's modulus, and elongation at break strongly depended on the degree of saponification. The average values of these properties are plotted against the degree of saponification in Figure 2.

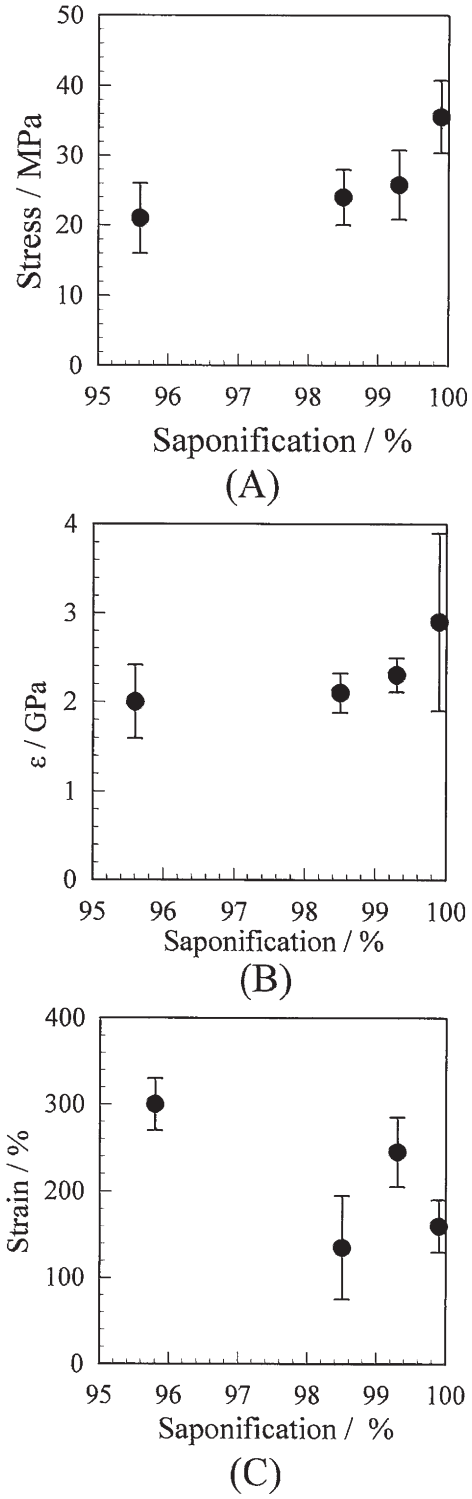

Figure 2. Tensile strength (A), Young's modulus (B), and the elongation at break (C) for CastF95.8, CastF98.5, CastF99.3, and CastF99.9 as a function of the degree of saponification.

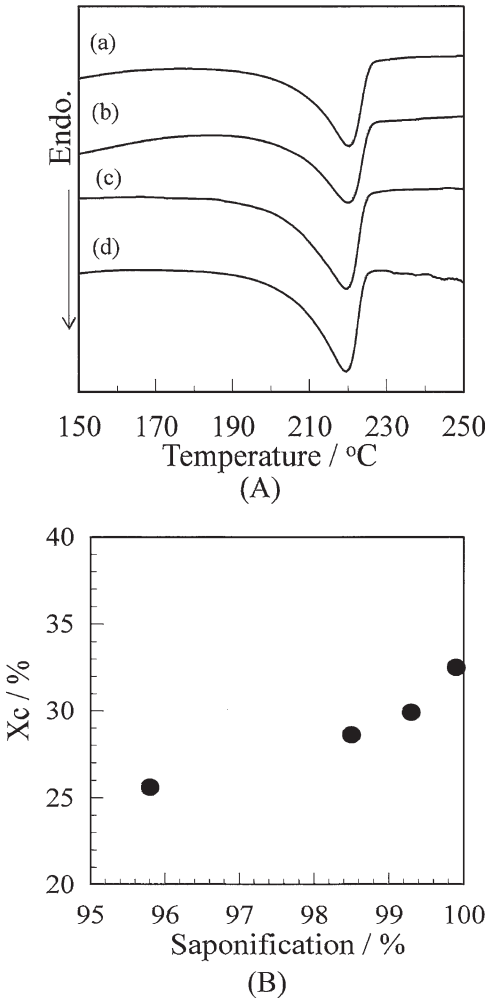

Figure 3. DSC chart (A) and the degree of crystallinity (B) as a function of saponification. (a) CastF95.8, (b) CastF98.5, (c) CastF99.3, and (d) CastF99.9.

The tensile strength and Young's modulus increased with increasing degree of saponification. The tensile strength of the CastF95.8 was as low as 20.8 ± 6.0 MPa, whereas CastF99.9 provided a tensile strength as high as 35.2 ± 6.0 MPa, which is about 1.8 times that of CastF95.8. Similarly, Young's modulus also increased from 2.0 GPa for CastF95.8 to 2.8 GPa for CastF99.9. These results show that the mechanical properties were improved by a higher degree of saponification. Samples with a higher degree of saponification have more hydroxy groups in their PVA chains. As the crystal is formed by hydrogen bonding, a higher crystallinity is expected for CastF99.9. In order to confirm this increase in crystallinity, DSC measurements were carried out. Figures 3(A,B) show a DSC chart and the degree of crystallinity of cast films, respectively. The melting temperatures were almost the same, but the melting enthalpy was larger for PVA with a higher degree of saponification. The crystallinity (X_c) was estimated from the observed melting enthalpy (ΔH_{obs}) as follows:

$$X_c = \frac{\Delta H_{obs}}{\Delta H_{100}} \quad (1)$$

Here, ΔH_{obs} denotes the melting enthalpy of 100% crystallinity, and adopted the value of 138.6 J/g.[20] The results were plotted in Figure 3(B). The crystallinity of CastF95.8 was 25.6%, but that of CastF99.9% was 32.5%. This resulted in good mechanical properties for CastF99.9.

The elongation at break decreased with increasing degree of saponification, as shown in Figure 2(C). Elongation involves the noncrystalline chains between crystallites. Because the crystallinity of CastF99.9 is high, there is less of the noncrystalline phase, so elongation is more difficult because of the shorter tie molecules between crystallites.

The CastF99.9 film provided the best mechanical properties of the four samples, so the mechanical properties of PVA99.9 will be discussed in the next section, based on films prepared via freeze/thaw cycling.

Mechanical Properties of PVA99.9 Films Prepared from Freeze/Thaw Cycled Gels

In our previous report, the mechanical properties of PVA with 98.5% saponification were measured.[19] We showed that films

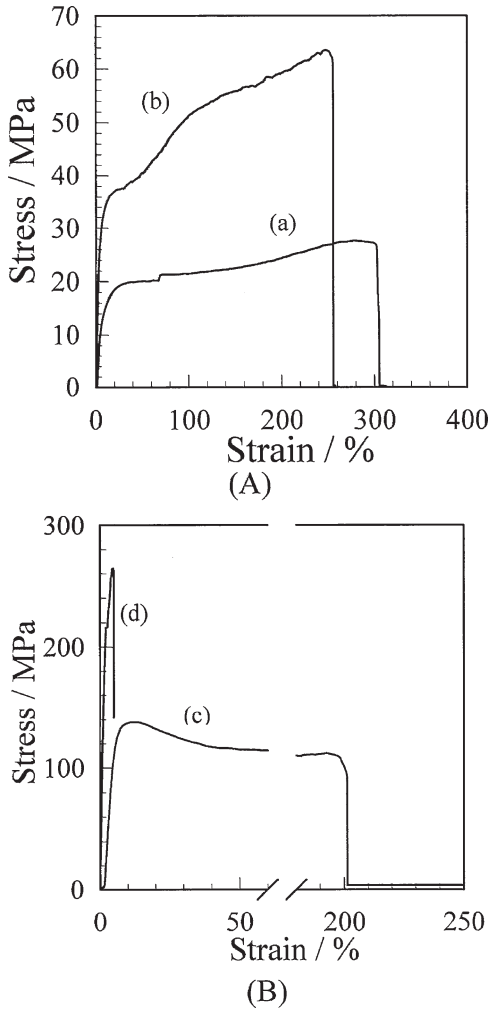

Figure 4. Typical stress–strain curves for CastF and GelF(7) before (A) and after (B) annealing at 130°C. (a) CastF99.9, (b) GelF99.9(7), (c) aCastF99.9, and (d) aGelF99.9(7).

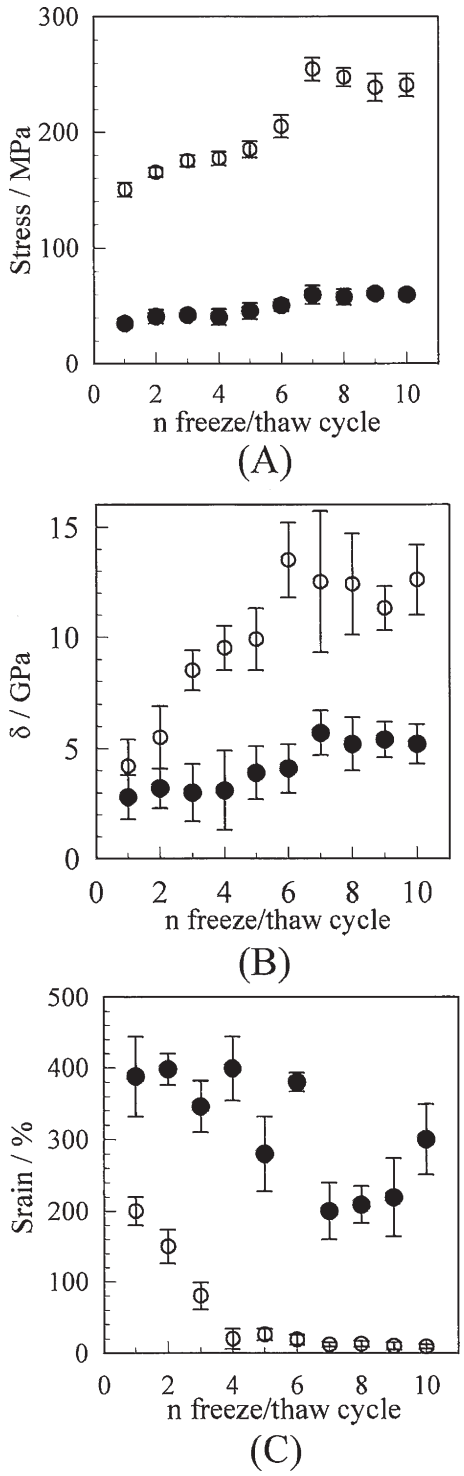

Figure 5. Tensile strength (A), Young's modulus (B), and elongation at break (C) as a function of degree of saponification. ●: before annealing, and ○: after annealing.

prepared from a freeze/thaw cycled gel provided much better mechanical properties than films cast from aqueous solution. In this section, the mechanical properties of PVA films with 99.9% saponification, prepared from freeze/thaw cycled gels, are analyzed and compared with those of the PVA98.5 film. Figures 4(A,B) show stress–strain curves for CastF99.9 and GelF99.9(7) before annealing, and aCastF99.9 and aGelF99.9(7) after annealing, respectively. There is a significant difference between films prepared with and without freeze/thaw cycling. The tensile strength of CastF99.9 was as low as 35.2 ± 6.0 MPa, whereas that of GelF99.9(7) was 60.4 ± 7.0 MPa. When films were annealed at 130°C, their tensile strength increased dramatically. The tensile strength of the aGelF99.9(7) was as high as 255 MPa, approximately four times that of GelF99.9(7) before annealing. The average tensile strength before and after annealing is plotted as a function of the number of freeze/thaw cycles in Figure 5(A). The tensile strength increased with increasing freeze/thaw cycles, and was almost constant around 250 MPa after seven freeze/thaw cycles. In the previously reported case of PVA98.5,[19] the highest tensile strength was 181 MPa for aGelF98.5(10), as summarized in Table I. In this study, the tensile strength was over 200 MPa. It is worth noting that there is no report of such a high tensile strength without the use of an additive.

Figure 5(B) shows Young's modulus as a function of the number of freeze/thaw cycles. A similar trend was observed; Young's modulus increased with increasing freeze/thaw cycles. Young's modulus before annealing increased from 2.8 GPa for CastF99.9 to 4.1 GPa for GelF99.9(7). After annealing, Young's modulus increased from 3.2 GPa for aCastF99.9 to 13.5 GPa for aGelF99.9(7). Young's modulus of aGelF99.9(7) film was four times that of the same film formed without freeze/thaw cycling. Young's modulus of aGelF98.5(7) was reportedly 8.9 GPa.[19] Therefore, Young's modulus for aGelF99.9(7) was almost 1.5 times that of the previous one.[19]

In Figure 5(C), the elongation at break is plotted against the number of freeze/thaw cycles. For GelF99.9 films, the elongation at break was reduced from 388% for GelF99.9(1) to 219% for GelF99.9(9). This is because the degree of crystallinity was higher. In contrast, the elongation at break of aGelF99.9(1) was 202%, which is about half that of GelF99.9(1). After four or more freeze/thaw cycles, the elongation at break was less than 30%. These results show that aGelF99.9 films formed after four freeze/thaw cycles were stronger and harder, with a lower elongation at failure.

Crystallinity for PVA with 99.9% Saponification

Thermal analysis was carried out to confirm the crystallinity of the samples. Figures 6(A,B) show DSC charts of GelF99.9 and aGelF99.9 with various numbers of freeze/thaw cycles. The observed melting temperature was around 220°C, irrespective of the number of freeze/thaw cycles, but the melting enthalpy increased with increasing freeze/thaw cycles. Figure 7 shows a plot of the crystallinity as a function of the number of freeze/thaw cycles. The crystallinity of CastF99.9 was as low as 32.5%, compared to 51.5% for GelF99.9(7). These differences arise from the molecular structure formed during the gelation process by the freeze/thaw cycling. Ricciardi et al. estimated the crystallinity of hydrogels prepared by a freeze/thaw cycle process using X-ray diffraction analysis, and reported that a PVA hydrogel consists of aggregated water, swollen PVA, and crystalline PVA. The crystallinity increased from 2.5% after 1 cycle to 6.3% after 9 cycles.[13] During the water evaporation process, the

Table I. Crystallinity, Mechanical Properties, and T_g for aCastF98.5, aGelF98.5(10), aCastF99.9, and aGelF99.9(7) Samples

	Crystallinity (%)	σ (MPa)	ε (GPa)	ΔL (%)	T_g (°C)
aCastF98.5[19)]	33.2	103.4 ± 14.3	2.6 ± 1.0	6.6 ± 2.0	58.6
aGelF98.5(10)[19)]	49.8	180.6 ± 9.8	8.9 ± 1.0	6.3 ± 3.7	74.1
aCastF99.9	53.5	123 ± 7.0	3.2 ± 0.9	211 ± 15.0	62.3
aGelF99.9(7)	70.0	255 ± 10.0	13.5 ± 3.2	12 ± 3.0	76.8

σ: Tensile strength, ε: Young's modulus, and ΔL: elongation at break.

crystallites formed in the gel act as nucleation sites. Therefore, a PVA film prepared using more freeze/thaw cycles tends to have a higher crystallinity. This resulted in good mechanical properties.

DSC profiles and the crystallinity after annealing are also shown in Figures 6(b) and 7, respectively. The crystallinity after annealing increased from 53.5% for aCastF99.9 to 75.2 % for aGelF99.9(8). Even without annealing, the crystallinity of GelF99.9(9) was as high as 55.8%. It is worth noting that the crystallinity of aGelF99.9(1) was 55.2%, which is comparable to that of GelF99.9(9), despite the additional freeze/thaw cycles for GelF99.9(9). Although the crystallinities were comparable, these films exhibited a large difference in their mechanical properties. Specifically, the tensile strength was 58 MPa for GelF99.9(8) and 123 MPa for aCastF. This suggests a difference in morphology between the two samples. In order to clarify the molecular morphology, X-ray diffraction measurements were performed.

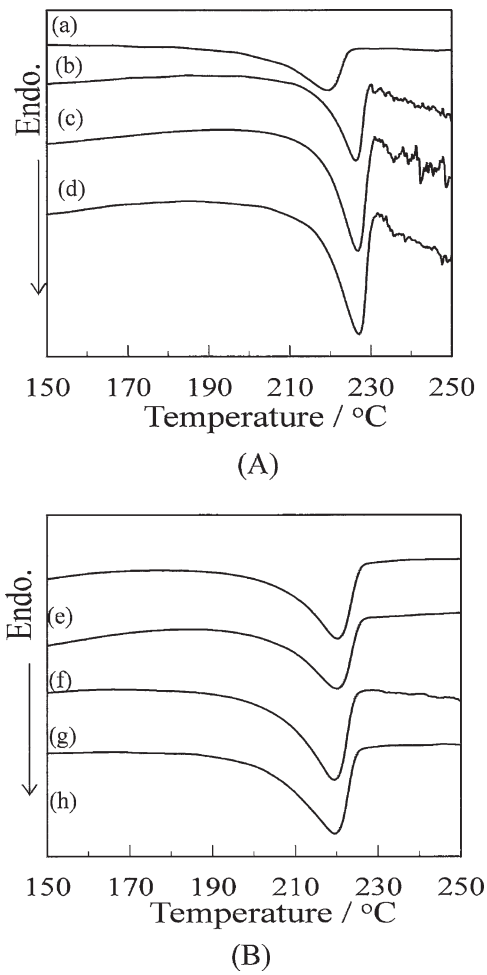

Figure 6. DSC charts before (A) and after (B) annealing at 130°C. (a) GelF99.9(2), (b) GelF99.9(4), (c) GelF99.9(6), (d) GelF99.9(8), (e) aGelF99.9(2), (f) aGelF99.9(4), (g) aGelF99.9(6), and (h) aGelF99.9(8).

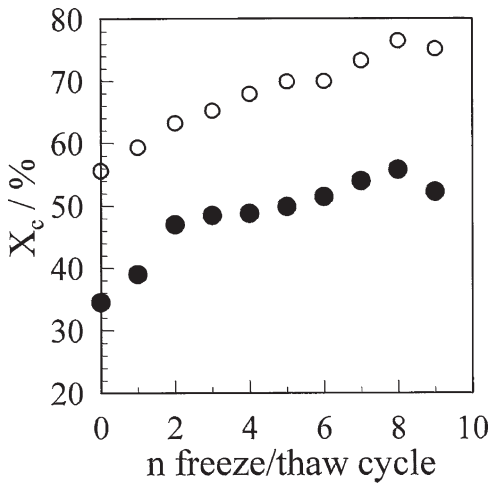

Figure 7. Degree of crystallinity before (●) and after (○) annealing at 130°C as a function of the number of freeze/thaw cycles.

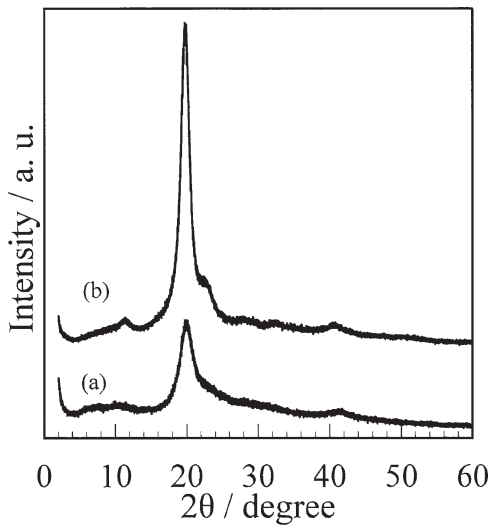

Figure 8. X-ray diffraction patterns of (a) GelF99.9(7) and (b) aGelF99.9(7).

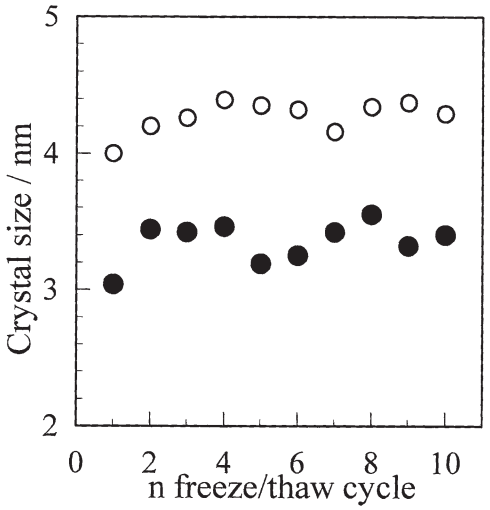

Figure 9. Crystal size estimated by Scherer's equation as a function of the number of freeze/thaw cycles. ●: before annealing and ○: after annealing.

Crystal Size Estimation by X-ray Diffraction

Figure 8 shows the X-ray diffraction patterns of GelF99.9(7) and aGelF99.9(7). A sharp crystalline peak was observed at $2\theta = 19.4°$ ($d = 4.68$ Å) assignable to the (010) plane. After annealing, this peak became much sharper. The crystal size (D) can be estimated from the full-width at half-maximum using Scherrer's equation:

$$D = \frac{K \cdot \lambda}{\gamma \cdot \cos\vartheta} \tag{2}$$

Here, K, λ, and β denote the Scherrer constant, the wavelength of the X-ray, and the full-width at half-maximum, respectively. The crystal size was estimated from the (010) peak. Figure 9 plots the crystal size as a function of number of freeze/thaw cycles. The crystal size increased slightly with increasing freeze/thaw cycles. On the other hand, a significant difference was observed before and after annealing. The crystal size before annealing was 3.0–3.5 nm, whereas after annealing it was 4.0–4.5 nm. As discussed in the previous section, Gel99.9(9) and aGel99.9(1) had almost the same degree of crystallinity, but their crystal sizes were 3.0 and 4.1 nm, respectively. After annealing, the crystals were about 1.4 times larger. This difference can be explained by considering the number and size of crystallites; small crystallites are dispersed before annealing, whereas larger crystallites are formed during annealing. Therefore, it was concluded that GelF99.9(9) has a large number of small crystallites, whereas aGelF99.9(1) has smaller number of large crystallites. This resulted in different mechanical properties before and after annealing.

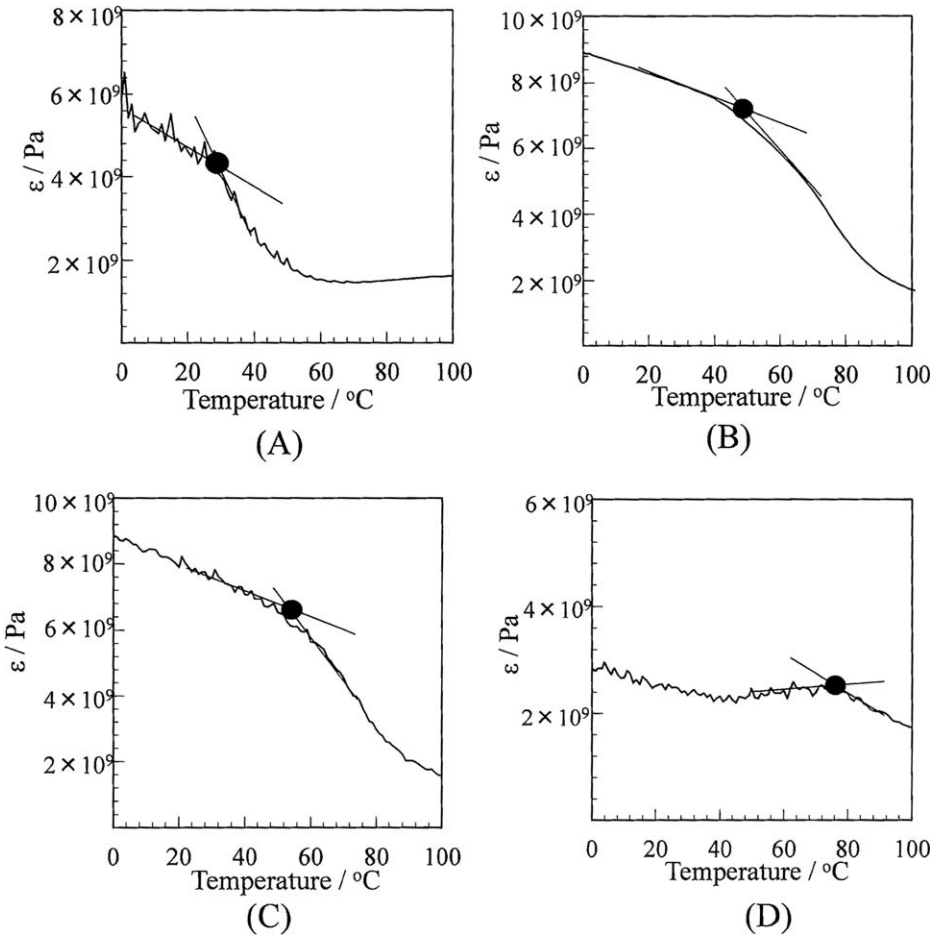

Figure 10. Storage modulus of (A) CastF99.9, (B) GelF99.9(7), (C) aCF99.9, and (D) aGelF99.9.

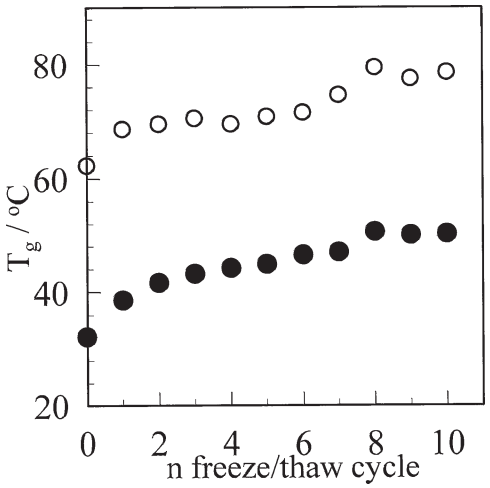

Figure 11. Glass transition temperature (T_g) before (●) and after (○) annealing at 130°C as a function of the number of freeze/thaw cycles.

Glass Transition Temperature of the Gel Films

Figures 10(A–D) show the storage modulus of CastF99.9, GelF99.7(7), aCastF99.9(7), and aGelF99.9(7), respectively, measured by DMA, and its dependence on temperature. The T_g of CastF99.9 was 32.2°C, whereas that of GelF99.9(7) was 46.5°C. As T_g represents the transition temperature from a glassy to a rubbery state, this difference is probably a result of the morphological structure of the noncrystalline chains. As shown in the previous section, a comparatively large number of crystallites are formed in GelF99.9(7) during the freeze/thaw cycles. In this case, the amorphous chains between the crystallites should be more distorted than in CastF99.9, leading to a higher T_g for GelF99.9(7). When the films were annealed, T_g increased for both aCF99.9 and aGelF99.9(7), as shown in Figures 10(C,D), respectively. Figure 11 shows a plot of T_g as a function of the number of freeze/thaw cycles. T_g increased with increasing freeze/thaw cycles, both before and after annealing. The T_g before annealing increased from 38.6°C for GelF99.9(1) to 50.6°C for GelF99.9(8), whereas after annealing it increased from 68.6°C for aGelF99.9(1) to 79.5°C for aGelF99.9(8). As more crystallites form during the freeze/thaw cycles, the noncrystalline chains should be more distorted, leading to a higher T_g. The annealing effect can be explained by the same reasoning.

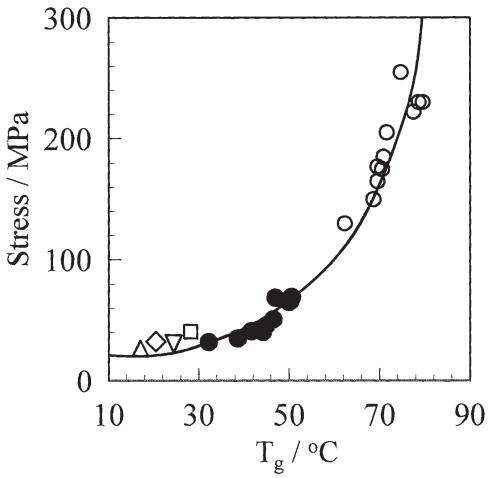

Figure 12. Relationship between the tensile strength and T_g for PVA with 99.9% saponification before (●) and after (○) annealing. The tensile strength of CastF95.8 (△), Cast98.5 (◇), CastF99.3 (▽), and CastF99.9 (□) are also shown.

It has been shown that the tensile strength and T_g for PVA with 98.5% saponification are related as follows[19]:

$$S_{max} = 0.050 T_g^2 + 1.2 T_g \quad (3)$$

where S_{max} denotes the tensile strength. Therefore, the tensile strength of PVA99.9 was plotted against T_g, as shown in Figure 12, and the experimental results were fitted to eq. (3). Furthermore, the tensile strengths of cast films with different degrees of saponification, as shown in Figure 2, were also plotted and fitted to eq. (3). The mobile component of the noncrystalline chain that results in a low T_g could be broken more easily. Therefore, it was concluded that the tensile strength can be fitted by expressed as a function of T_g, irrespective of both the degree of saponification and the annealing conditions.

CONCLUSIONS

The dependence of the mechanical properties of PVA films on the degree of saponification and the number of freeze/thaw cycles applied before forming the films from gels by water evaporation were investigated. The CastF99.9 film provided the highest tensile strength and Young's modulus and the lowest elongation at break out of 4 PVA films with different degrees of saponification. Therefore, a PVA film with 99.9% saponification was prepared from a freeze/thaw cycled hydrogel in order to investigate the mechanical properties as a function of the number of freeze/thaw cycles. The tensile strength and Young's modulus increased with increasing freeze/thaw cycles. After annealing at 130°C, these values for aGelF99.9(7) were as large as 255 MPa and 13.5 GPa, respectively. Note that no additives were used. The elongation at break decreased with increasing freeze/thaw cycles, because the crystallinity increased with increasing freeze/thaw cycles.

The crystal size was observed by X-ray diffraction, and increased slightly with increasing freeze/thaw cycles; from 3.0–3.5 nm before annealing to 4.0–4.5 nm after annealing. GelF99.9(9) and aGelF99.9(1) had similar crystallinity, but their crystal sizes were different: 3.3 and 4.1 nm, respectively. This indicates that the number of crystallites is higher in GelF99.9(9). This morphological difference resulted in different mechanical properties.

The tensile strength and T_g were fitted by eq. (3). This relationship is irrespective of both the degree of saponification and annealing conditions. In other words, the tensile strength only depends on the amorphous state. A high T_g corresponds to the presence of rigid amorphous chains between the crystallites, resulting in a higher tensile strength.

ACKNOWLEDGMENTS

The authors thank Dr. Ohgi of Kuraray for kindly providing the PVA sample.

REFERENCES

1. Konidari, M. V.; Papadokostaki, K. G.; Sanopoulou, M. *Appl. Polym. Sci.* **2011**, *120*, 3381.
2. Mbhele, H.; Salemane, M. G.; van Sittert, C. G. C.; Nedeljkovic, J. M.; Djokovic, V.; Luyt, A. S. *Chem. Mater.* **2003**, *15*, 5019.
3. Johnsy, G.; Datta, K. K. R.; Sajeevkumar, V. A.; Sabapathy, S. N.; Bawa, A. S.; Eswaramoorthy, M. *Appl. Mater. Interfaces* **2009**, *12*, 2796.
4. Zhao, X.; Zhang, Q.; Chen, D. *Macromolecules* **2010**, *43*, 2357.
5. Zhang, X.; Liu, T.; Sreekumur, T. V.; Kumar, S.; Moore, V. C.; Hauge, R. H. *Nano Lett.* **2003**, *3*, 1285.
6. Morimune, S.; Kotera, M.; Nishino, T.; Goto K.; Hata, K. *Macromolecules* **2011**, *44*, 4415.
7. Podsiadlo, P.; Kaushik, A. K.; Shim, B. S.; Agarwal, A.; Tang, Z.; Waas, A. M.; Arruda, E. M. *J. Phys. Chem. B* **2008**, *112*, 14359.
8. Prasad, K. E.; Das, B.; Maitra, U.; Ramamurty, U.; Rao, C. N. R. *Proc Natl Acad Sci USA* **2009**, *106*, 13186.
9. Peppas, N. A. *Makromol. Chem.* **1975**, *176*, 3433.
10. Hassan, C. M.; Peppas, N. A. *Adv. Polym. Sci.* **2000**, *153*, 37.
11. Lozinsky, V. I. *Russ. Chem. Rev.* **1998**, *67*, 573.
12. Lozinsky, V. I.; Galaev, I. Y.; Plieva, F. M.; Savina, I. N.; Jungvid H.; Mattiasson, B. *Trends Biotechnol.* **2003**, *21*, 445.
13. Ricciardi, R.; Auriemma, F.; De Rosa C.; Laupretre, F. *Macromol.* **2004**, *37*, 1921.
14. Ricciardi, R.; Auriemma, F.; Gaillet, C.; De Rosa, C.; Laupretre, F. *Macromolecules* **2004**, *37*, 9510.
15. Ricciardi, R.; Mangiapia, G.; Lo Celso, F.; Paduano, L.; Triolo, R.; Auriemma, F.; De Rosa C.; Laupretre, F. *Chem. Mater.* **2005**, *17*, 1183.
16. Willcox, P. J.; Howie, D. W.; Shimidt-Rohr, K.; Hoagland, D. A.; Gido, S. P.; Pudjijanto, S.; Kleiner, L. W.; Venkatraman, S. J. *J. Polym. Sci. B* **1999**, *37*, 3438.
17. Nakaoki, T.; Yamashita, H. *J. Mol. Struct.* **2008**, *875*, 282.
18. Nakano, T.; Nakaoki, T. *Polym J* **2011**, *43*, 875.
19. Fukumori, T.; Nakaoki, T. *Open J. Org. Polym. Mater.* **2013**, *3*, 110.
20. Hickey, A. S.; Peppas, N. A. *Membr. Sci.* **1995**, *107*, 229.